8 Contrast-Enhanced Ultrasound: The Current State

M. Beth McCarville, Annamaria Deganello, and Zoltan Harkanyi

8.1 Introduction

Ultrasound (US) imaging in children has been a widely accepted and routinely used imaging modality for many decades. In fact, in many clinical scenarios, US is the preferred, first-line imaging modality to be performed. The attributes of US, particularly in pediatrics, are many; it is noninvasive, child-friendly, and portable, provides Doppler capabilities for vascular interrogation, does not require sedation, and most importantly does not expose the patient to the potentially harmful effects of ionizing radiation. The avoidance of radiation and sedation is particularly relevant in pediatric oncology because children with cancer undergo innumerable imaging examinations for diagnosis and staging, during therapy to monitor treatment response and to assess acute and chronic complications of therapy and then during surveillance for years after completion of therapy. A recent study from Great Britain showed an association between radiation exposure from CT scans and an increased risk of developing brain tumors and leukemia in children [1]. In that study the reported brain tumor risk was comparable to observed risk estimates for brain tumors following childhood radiation exposure in Japanese atomic bomb survivors. These findings underscore the importance of minimizing radiation exposure in children whenever possible.

Although US is often useful in identifying pathology in the abdomen, pelvis, pleural spaces, and extremities, image resolution of B-mode US is limited, and further cross-sectional imaging with CT or MRI may be required. In addition to radiation exposure and sedation, these additional tests add cost, can create anxiety, and frequently necessitate the administration of an intravenous contrast agent. There are risks associated with the iodinated contrast agents used for CT and gadolinium-based contrast agents used for MRI. Neither of these types of contrast agents can be safely administered in patients with renal insufficiency due to the risk of nephrotoxicity and nephrogenic systemic fibrosis, respectively. Recently, gadolinium contrast agents have come under increased scrutiny for the yet unknown, but potential, long-term effects associated with gadolinium deposition in the brain and other solid organs [2]. Unlike the very small molecules that

M. B. McCarville (✉)
Department of Diagnostic Imaging, St. Jude Children's Research Hospital, Memphis, USA
e-mail: beth.mccarville@stjude.org

A. Deganello
Department of Radiology, King's College Hospital, London, UK
e-mail: adeganello@nhs.net

Z. Harkanyi
Department of Radiology, Heim Pal Children's Hospital, Budapest, Hungary

S. D. Voss, K. McHugh (eds.), *Imaging in Pediatric Oncology*, Pediatric Oncology,
https://doi.org/10.1007/978-3-030-03777-2_8

constitute iodinated and gadolinium-based contrast agents, ultrasound contrast agents (UCAs) are comprised of microspheres approximating the size of red blood cells. Due to their size, UCAs remain in the vascular space and, because they are not metabolized by the kidneys, can be safely administered to patients with renal insufficiency. Numerous reports have shown that these contrast agents have a high safety profile in adults and there is a growing body of literature showing similar safety in children [3–9]. A position statement issued by the European Federation of Societies for Ultrasound in Medicine and Biology, published in 2016, stated: "The evidence to date suggests that the safety profile of UCA in adults is good, and comparable to contrast agents used in MR imaging, better than the contrast agents in CT imaging. The more limited safety data in children suggests that UCA are as safe in children as in the adult population" [10]. Importantly, in 2016 the United States Federal Drug Administration (FDA) approved the first UCA for intravenous use in children to evaluate liver lesions and intravesical administration to assess for vesicoureteral reflux.

The addition of a contrast agent to ultrasound imaging offers the opportunity to improve lesion conspicuity and diagnostic confidence and could obviate the need for additional cross-sectional imaging in some circumstances. The use of UCAs in adult practices is well established in Europe and is increasing in North America. The expansion of CEUS into pediatric applications has lagged behind, primarily because of the lack of regulatory approval and limited clinical experience outside of large academic centers. With the recent US FDA approval of a UCA for children, coupled with an increasing emphasis on medical cost containment and radiation reduction, the time is ripe for the development of this important alternative imaging modality in routine pediatric clinical practice. In this chapter we will discuss the essential technical and safety features that are vital to the successful performance of CEUS in children. Although the role of CEUS in pediatric oncology is currently somewhat limited, we will present examples illustrating the value of CEUS in this setting, particularly with regard to pediatric liver lesions. Finally, we will discuss future directions and potential applications of CEUS in the diagnosis and management of pediatric malignancies.

8.2 Safety Considerations of CEUS Studies

All current UCAs consist of a gas surrounded by a thin encapsulating shell. The most widely used UCA is sulfur hexafluoride with a phospholipid shell (SonoVue/Lumason®, Bracco, Milan, Italy), which was introduced in 2001 and approved by the US FDA for pediatric intravenous (IV) and intravesical use in 2016. In the United States, there are two additional UCAs that are approved only for adult cardiac studies: Definity® (Lantheus Medical Imaging, Billerica, MA), which is comprised of octafluoropropane encapsulated in a phospholipid shell, and Optison™ (GE Healthcare, Princeton, NJ), an octafluoropropane gas within an albumin shell. There are no data regarding pediatric applications of Sonazoid (GE Healthcare, Oslo, Norway), a hepatocyte-specific agent composed of perfluorobutane gas within a phospholipid shell, that is widely used in Asia [10, 11].

The safety profile of SonoVue/Lumason® UCA during intravenous administration has been documented in a large cohort of 23,188 adults with no fatal event encountered and only 29 adverse reactions noted (three severe, three moderate, and 23 mild) [12]. The overall rate of adverse events (0.0086%) was comparable to the administration of contrast media used in MR imaging (0.0088%) and lower than iodinated contrast media used in CT imaging (0.6%) [10]. The safety profile of UCAs in children is based on limited but growing information. Three dedicated safety studies have included vital signs monitoring, while using UCA containing a perfluorocarbon gas [5, 9, 13]. In a study of 13 children who underwent IV CEUS with escalating doses of Optison™ based on body surface area, three children experienced mild adverse events; two had altered taste and one mild tinnitus and light-headedness [13]. In a further study by the same group, 134 CEUS examinations in 34 children (median age 8.7 years) were evaluated, reporting a lower frequency of similar mild

adverse reactions [5]. In a study of 20 children (median age 15 years) receiving Optison™, four experienced adverse reactions; three developed a transient headache and one reported brief taste alteration [9]. A sulfur hexafluoride gas containing UCA was also evaluated in a dedicated safety study of 167 intravenous CEUS investigations in 137 children (median 10.2 years) [4]. In that study, a single patient (0.6%) suffered severe anaphylactic shock that was potentially life threatening and directly related to the IV UCA administration. Management consisted of oxygen, IV epinephrine, and fluids (0.9% NaCl) with resolution in 2 h. In a survey of radiologists from 29 European centers, there were 948 CEUS examinations performed in children with intravenous sulfur hexafluoride gas-filled UCA. Five minor adverse events were reported which included skin reaction, altered taste, and hyperventilation [14].

Ultrasound contrast agents are not metabolized by the kidneys, and there is no evidence of nephrotoxicity associated with their use. Therefore, unlike iodinated and gadolinium-based contrast agents, UCAs can be safely administered to patients with poor renal function. However, a drawback is that UCAs cannot be used to evaluate the renal collecting system when they are administered intravenously.

History of a hypersensitivity reaction to any of the ingredients in UCAs is a contraindication to their use. During CEUS studies one must always be prepared to manage an adverse reaction. Resuscitation facilities including appropriate drugs must be available in the examination room, and a second person must be present during the study.

8.3 Technical Considerations of CEUS Studies

The radiologist must clearly define the goal of the CEUS study before its performance. It is almost always a focused study in order to answer a specific diagnostic question. Basic training in B-mode and color Doppler techniques are essential prerequisites for those wishing to perform contrast studies.

8.3.1 Checklist for Performance of a CEUS Examination [11]

1. Examination and documentation of the region of interest with B-mode and color Doppler US.
2. Review of any prior imaging studies (US/CEUS/MR/CT). This is of utmost importance in long-term follow-up of pediatric oncology patients to better characterize the lesion of interest.
3. Determine whether a CEUS study is indicated for the diagnostic question.
4. Assess patient for any contraindication to CEUS.
5. Have a second person present during the CEUS study to inject and monitor the patient.
6. Ensure that treatment and life support are available for allergic reactions to UCA.
7. Obtain informed consent (verbal or written as per local institutional practice) from parents or patient as appropriate.
8. Determine dose of UCA and saline flush and verify contrast agent expiration date.
9. Use a needle of 20–24 gauge for IV. If the needle caliber is too small, it may result in microbubble destruction.
10. Ensure capability of US machine to record video clips during the CEUS study.
11. Be certain that the contrast-specific software within the US scanner is functional.
12. Select appropriate US probe and scanning parameters for CEUS study.
13. Start timer at the moment of injection.
14. Start recording cine loop after the arrival of the first bubbles for approximately 20–40 s, and then record in the venous and late phase using short clips while scanning the whole organ. Store images and video clips (e.g., picture archive and communication system [PACS], DVD, CD).
15. Review the study at a PACS workstation using stored images and cine clips and report the examination.

The dose of UCA generally can be determined by the patients' age or weight depending on the agent being used [3, 9]. When using SonoVue/Lumason® to perform a liver CEUS study on a

child, the following doses are suggested: between the age of 0 and 6 years, 0.6 mL; 6–12 years, 1.2 mL; and between 12 and 18 years, 2.4 mL. Recommended doses for Optison™ are 0.3 mL for patients less than 20 kg and 0.5 mL for others [9]. However, doses may need to be adjusted depending on the size and body habitus of the patient, depth of the lesion, underlying diffuse hepatic parenchymal disease, type of transducer (convex or linear), and the CEUS software version of the ultrasound system. In the case of multiple parenchymal lesions (liver, kidney) or when the characterization of a lesion remains questionable, repeat injections can be performed as needed after allowing the first dose to clear the circulation (generally about 10 min). The manufacturer's maximum cumulative dose recommendation can be found in the package insert and should be adhered to. The quality of CEUS studies has significantly improved with the introduction of contrast-specific software; however, the sensitivity to display microvascularity (presence of microbubbles at the capillary level) can vary between US systems.

Imaging parameters, such as the mechanical index (MI) and position of the focal zone, should be adjusted at the beginning of the CEUS study according to the diagnostic question. The use of a split screen, with a grayscale image on one side and the corresponding CEUS image on the other, is quite helpful to maintain the proper scanning plane during the study. In the later phase of imaging, the CEUS display alone may be sufficient to depict the lesion(s) and allows viewing of a larger area of anatomy. The average time required to perform a CEUS study in experienced hands is 15–25 min, including preparation of the UCA.

8.4 Contrast-Enhanced Ultrasound Imaging Features of Pediatric Malignancies

To be incorporated into the routine management of oncology patients, CEUS will need to demonstrate added value or improved diagnostic performance over existing imaging modalities. The added value of CEUS, and its accuracy relative to CT and MRI, has perhaps been best described in the assessment of liver lesions. In a study of 147 adult patients by D'Onofrio and colleagues, the late phase of CEUS was compared to the hepatobiliary phase of contrast-enhanced MRI for distinguishing benign from malignant liver lesions. Contrast-enhanced ultrasound had a sensitivity, specificity, positive predictive value (PPV), negative predictive value (NPV), and accuracy of 90%, 93%, 97%, 80%, and 91% compared to 91%, 93%, 97%, 81%, and 92%, respectively, by MRI and rose to 98%, 98%, 99%, 95%, and 98%, respectively, when findings from both modalities were considered concurrently [15]. Similar findings were reported by Quaia et al., who compared CEUS to contrast-enhanced CT (CE-CT) in 46 non-cirrhotic adults with 55 liver lesions. In that study, the sensitivity, specificity, PPV, NPV, and accuracy for two reviewers were superior for CEUS compared to CE-CT and improved when CEUS and CE-CT images were reviewed concurrently [16]. In a study of 134 adult patients with focal liver lesions (FLLs) who underwent CEUS and contrast-enhanced CT and/or MRI, Trillaud and colleagues found that CEUS had a sensitivity, specificity, and accuracy of 98%, 88%, and 93% compared to 69%, 79%, and 72%, respectively, for CT/MRI. Thirty patients in their study underwent biopsy; compared to pathology CEUS had a sensitivity, specificity, and accuracy of 96%, 75%, and 90% compared to 73%, 38%, and 63% for CT and 82%, 43%, and 67% for MRI [17].

There are a small number of studies dedicated to the role of CEUS in focal liver lesion (FLL) characterization in pediatrics [4, 6, 8, 18, 19]. In a study of 44 children with indeterminate FLLs on grayscale ultrasound, investigators compared CEUS with consensus cross-sectional imaging or histology as the gold-standard method and showed agreement in 85% of cases [6]. A more recent dedicated pediatric study compared CEUS to CT and MR of 60 liver lesions and anomalies of portal vein perfusion. CEUS was able to differentiate accurately between benign and malignant lesions and could characterize 45 out of 49 FLLs; MRI and CEUS findings were concordant

in 84% of the cases and CT and CEUS were concordant in five out of eight cases. In 21 lesions CEUS was the only imaging modality used to characterize the lesions and was deemed sufficient to achieve a diagnosis [19].

A study by Smith et al. showed that the incidence of new focal liver lesions in 273 children treated for a solid malignancy who were followed with abdominal imaging was 17% [20]. When such lesions arise in a child with a history of underlying malignancy, there is always a concern for metastatic recurrence. Given the body of evidence supporting the use of CEUS to distinguish benign from malignant liver lesions, in conjunction with the recent FDA approval of a UCA for assessment of the liver in children, this modality should be given high priority in the management of these patients. Taken together, the high spatial resolution of ultrasonography and the accuracy of CEUS in determining the nature of a FLL, CEUS could become the modality of choice to identify and characterize small liver lesions [21].

The assessment of pediatric FLLs with CEUS does not differ from the adult population. The purely intravascular nature of the UCA gives the examiner the opportunity to visualize in real time the vascular enhancement of a lesion during the arterial, portal venous, and late phases. During the arterial phase, it is important to establish the position of initial enhancement within the lesion (central, eccentric, or peripheral) and the pattern of vascularization (uniform, stellate/spoke wheel, haphazard, globular, or peripheral rim). During the portal venous and late phases, the examiner needs to establish whether the lesion fills in or retains contrast or, conversely, if there is washout of contrast from the lesion. Contrast washout is a feature that is usually indicative of malignancy [15]. Some benign lesions, such as focal nodular hyperplasia (FNH) and hemangiomas (Fig. 8.1), have specific patterns of enhancement in the arterial phase (spoke wheel, centrifugal, or globular peripheral, respectively). Benign lesions typically remain iso- or hyperenhancing (Fig. 8.2) or continue to fill in during the portal venous and late phases (Fig. 8.1). Focal nodular hyperplasia may exhibit a central, non-enhancing scar (Fig. 8.3). Therefore, the enhancement patterns of these lesions can be established readily allowing a quick and accurate diagnosis. This is especially desirable in examining a child because it obviates the need for radiation exposure, sedation, and iodinated or gadolinium-based contrast infusion. An added, important benefit is that this approach allows immediate feedback to the patient/caregiver, thus alleviating the anxiety associated with additional imaging and a delayed diagnosis.

Primary liver tumors are uncommon in children, and the majority are benign [22, 23]. Benign lesions can, nevertheless, undergo malignant transformation. The most common primary malignant liver tumor in children is hepatoblastoma. Others include hepatocellular carcinoma (HCC), embryonal sarcoma, and rhabdomyosarcoma. In children with chronic liver disease, the progression toward cirrhosis increases the risk of developing HCC, and these patients require close follow-up [11, 24].

On CEUS primary liver malignancies such as HCC and hepatoblastoma both display early disorganized vessels and hyperenhancement (Fig. 8.4) in the arterial phase. During the portal venous phase, hepatoblastoma tends to have rapid washout of contrast, whereas HCC (Fig. 8.5) may show hypoenhancement or slow washout only during delayed phase imaging depending on the degree of differentiation of the tumor. Undifferentiated embryonal sarcoma (UES) of the liver is a rare mesenchymal tumor of childhood but represents the third most common primary hepatic neoplasm after hepatoblastoma and HCC [25]. On CEUS, UES (Fig. 8.6) may display a hyperenhancing rim (thought to represent a fibrous pseudocapsule on pathology), with lack of internal enhancement during the arterial phase, followed by heterogeneous internal nodular enhancement in the late phase and late, faint washout of the peripheral rim.

Rhabdomyosarcoma of the liver is another rare malignant tumor but represents the most common biliary tract tumor in children; it often arises from the common bile duct (but can arise anywhere along the biliary tree) and, on B-mode ultrasound, presents as a solid mass occupying the bile duct lumen (Fig. 8.7), with or without

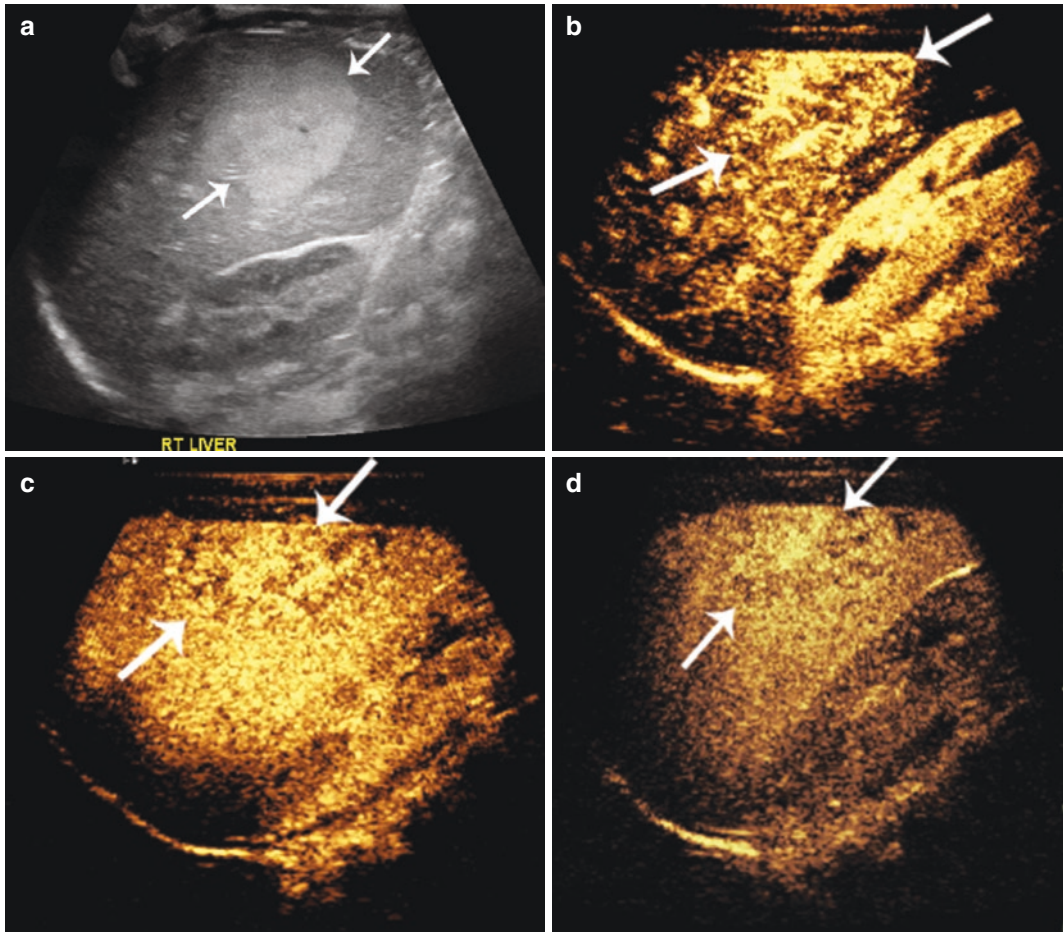

Fig. 8.1 A 3-month-old boy underwent an ultrasound to assess for pyloric stenosis and was incidentally found to have a liver lesion. (**a**) Sagittal grayscale ultrasound shows a large hyperechoic lesion in segments 5 and 6 of the liver (arrows). (**b**) Sagittal contrast-enhanced ultrasound (CEUS) image obtained in early arterial phase shows peripheral, globular enhancement of the lesion (arrows). (**c**) Sagittal portal venous phase CEUS shows centripetal enhancement of the lesion (arrows). (**d**) Sagittal delayed phase CEUS shows persistent, somewhat globular, central hyperenhancement of the lesion (arrows). These CEUS features are typical of hemangioma

extension into the liver parenchyma. On CEUS, like other imaging modalities, this lesion does not have specific features [26]. In our limited experience, this lesion has CEUS features similar to other liver malignancies, with variable arterial contrast enhancement and early washout in the portal venous phase (Fig. 8.7).

Metastases can either be hypoenhancing in all phases, hyperenhancing in the arterial phase, or hypoenhancing in the portal venous and late phases (Fig. 8.8) or show a rim of arterial enhancement followed by washout in the portal venous and late phases.

When assessing liver lesions, it is crucial to continue intermittent scanning for at least 4 min, to avoid missing late washout and misdiagnosing a malignant lesion as benign. Hyperenhancing metastases, some malignant mesenchymal primaries, and well-differentiated HCC may not demonstrate washout until 4–5 min after injection [27–29]. Therefore, caution and technique tuning (such as image freezing and intermittent scanning) must be applied to avoid microbubble destruction caused by the insonating sound waves and artifactual loss of enhancement that could precede contrast washout. It should be

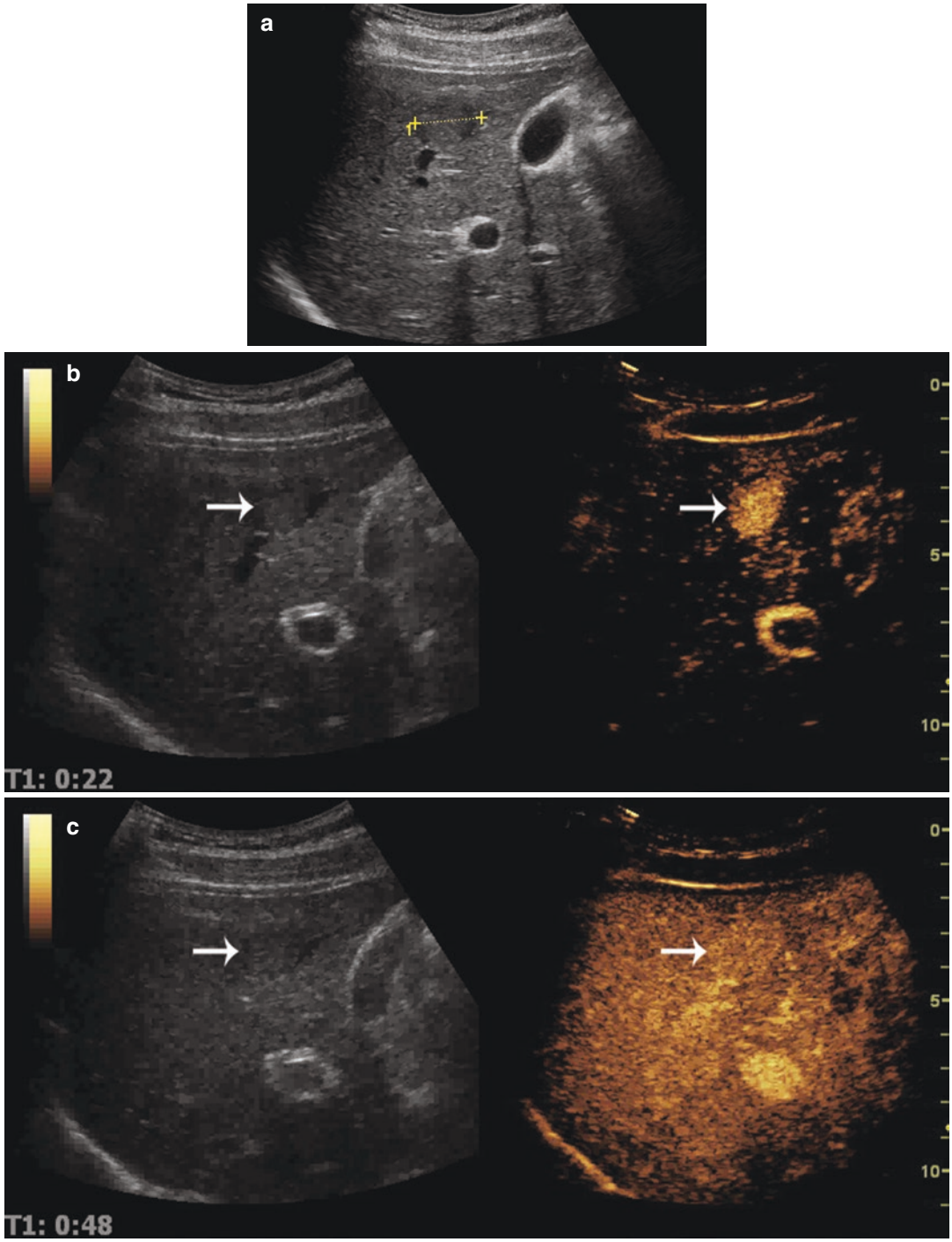

Fig. 8.2 An 18-year-old boy with cystic fibrosis. (**a**) Sagittal grayscale ultrasound image of the liver shows a mass in segment 5 (cursors). Sagittal CEUS images (right side of panels) (**b**) show the mass to be hyperenhancing in the arterial phase (arrows) (**c**) and isoenhancing in the delayed phase (arrows) with no evidence of washout. Clinical follow-up and MR imaging (not shown) were suggestive of hepatic adenoma

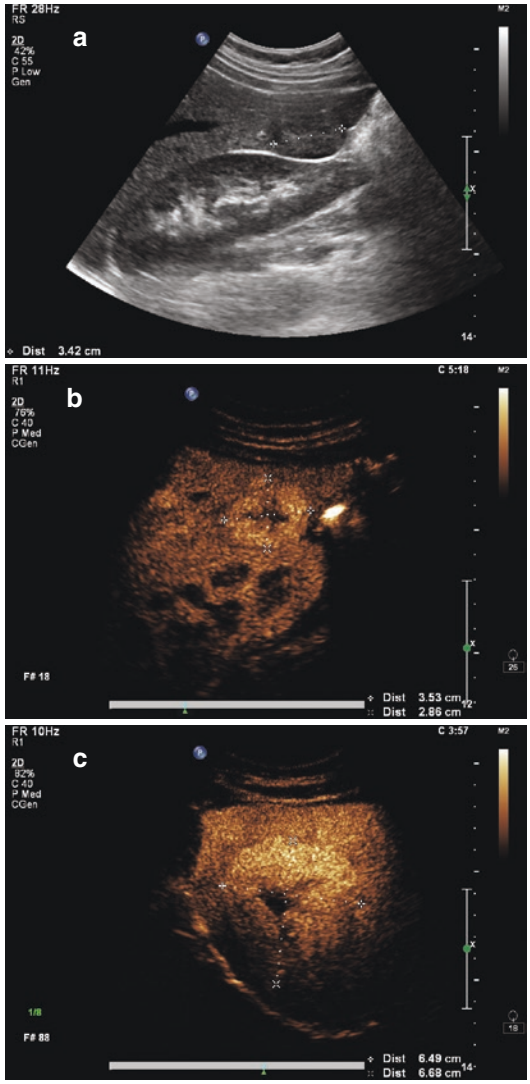

Fig. 8.3 A 17-year-old girl with history of treated neuroblastoma and multiple focal nodular hyperplasia (FNH) nodules. (**a**) Conventional sagittal grayscale ultrasound image shows a hypoechoic solid nodule in segment 6 of the liver (cursors). (**b**) Sagittal contrast-enhanced ultrasound (CEUS) image obtained during the portal venous phase shows the nodule is hyperenhancing and has a central scar (cursors). (**c**) A second, larger FNH in segments 7 and 8 (cursors) shows similar enhancement features. The lesions did not wash out on delayed phase imaging. These CEUS features are typical of FNH

remembered that no imaging modality is 100% accurate all of the time. There are reported cases of benign lesions, including adenomas and FNH, showing hypoenhancement in the late phase which was due to scarring or inflammation [6, 30]. Therefore, CEUS findings must be correlated with the clinical scenario and the index of suspicion for malignancy. When the CEUS and clinical findings are equivocal or conflicting early follow-up, alternative imaging modalities or biopsy may be needed as clinically indicated.

Non-hepatic oncology applications of pediatric CEUS is an expanding field with only a limited number of publications that are mainly focused on its safety profile [3, 5]. There are only sporadic case reports of the value of CEUS to aid the diagnosis of solid tumors [31]. An important, potential application of CEUS in pediatric oncology is establishing solid tumor resectability by defining tumor margins and identifying possible local vascular invasion [13]. The optimal spatial and temporal resolution of CEUS may make it the ideal tool for this purpose, especially in cases where CT and MRI are ambiguous. Likewise, CEUS can identify viable tissue within a solid lesion, to target biopsy and facilitate accurate sampling. Intravenous renal applications of CEUS have been evaluated in adults and can be applied to the pediatric population. These include differentiation between benign and malignant lesions and characterization of complex renal cysts [32]. CEUS has also proved to be useful in the evaluation of testicular lesions. Preliminary studies focused on CEUS time-intensity curves show its potential in discriminating Leydig cell tumors from seminomas on the basis of differing vascularity [33]. This could prove extremely useful in adolescent boys with the aim of testis sparing surgery.

8.5 Future Directions

The role of CEUS in oncology is rapidly expanding and evolving. There are a wide variety of potential applications of CEUS in the management of adult and pediatric oncology patients. Due to the relative rarity of pediatric malignancies, much of the clinical research in this area is occurring in the adult population. In addition to the malignancies already discussed, investigators have reported the value of CEUS in distinguishing benign from malignant thyroid nodules,

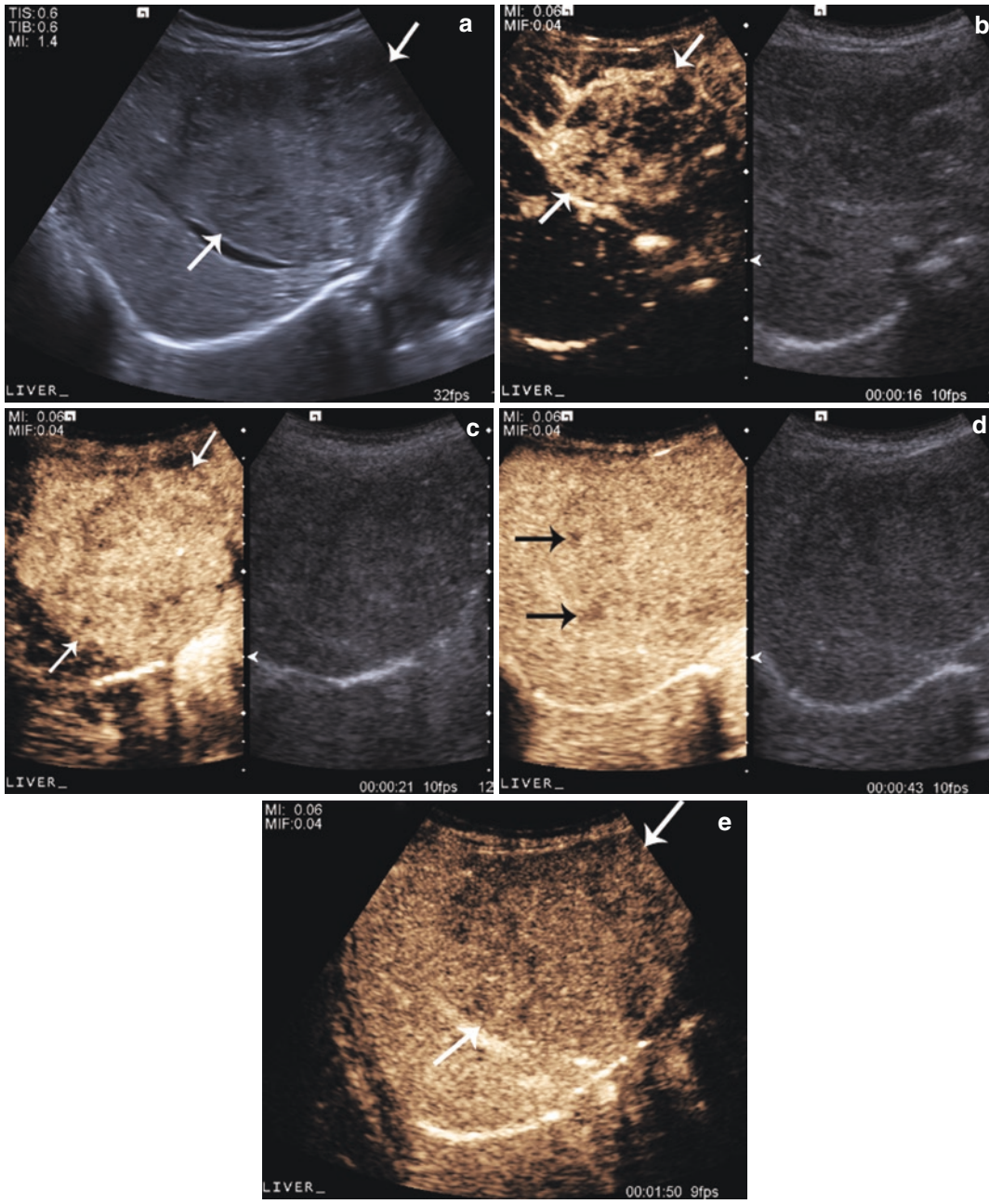

Fig. 8.4 A 2-year-old girl with hepatoblastoma. (**a**) Transverse grayscale ultrasound image showing primary tumor in segments 8 and 4A of the liver (arrows). (**b**) Transverse CEUS image (left side of panel) obtained in the early arterial phase shows hyperenhancement of tumor (arrows) with disorganized feeding vessels. (**c**) Transverse CEUS image (left side of panel) obtained in the late arterial phase shows diffuse hyperenhancement of tumor (arrows). (**d**) Transverse CEUS image (left side of panel) obtained at 43 s after injection shows early washout of contrast in some areas of the tumor (arrows). (**e**) At approximately 2 min after injection, there is continued washout of contrast throughout the tumor (arrows). These features are consistent with a malignant lesion

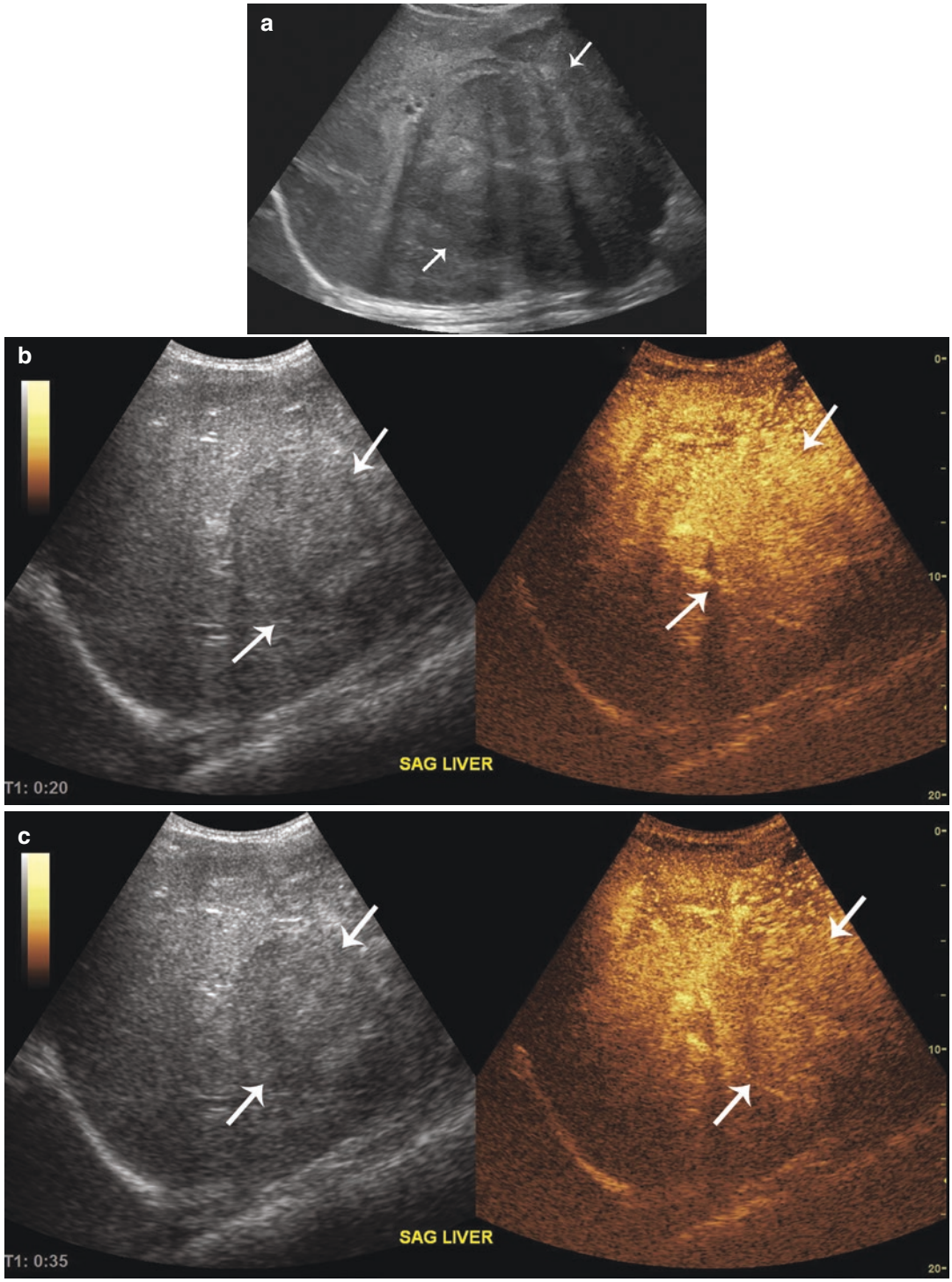

Fig. 8.5 A 15-year-old boy with palpable right upper quadrant mass proven by biopsy to be fibrolamellar hepatocellular carcinoma (HCC). (**a**) Transverse grayscale image shows large intrahepatic tumor (arrows). Transverse CEUS images (right side of panels) in the (**b**) early arterial phase shows hyperenhancement of the tumor (arrows). (**c**) In the portal venous phase, the tumor is isoenhancing (arrows), and (**d**) 1 min after injection, the tumor shows washout of contrast agent (arrows). These CEUS features are typical of HCC

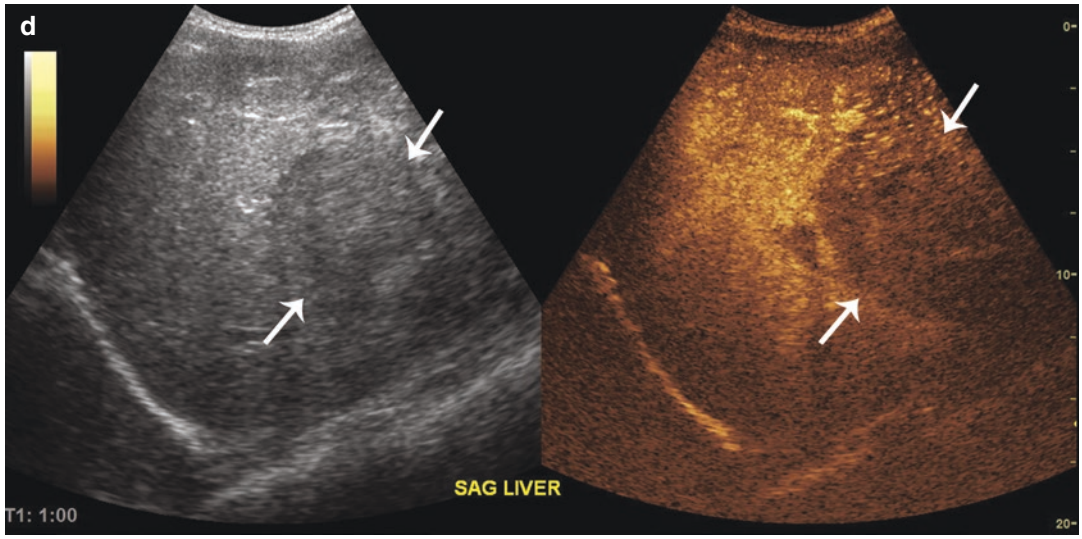

Fig. 8.5 (continued)

distinguishing endometrial hyperplasia from neoplasms, distinguishing benign from malignant soft tissue masses, differentiating low- from high-grade bladder carcinoma, distinguishing benign from malignant lymph nodes, distinguishing prostate carcinoma from benign prostatic hypertrophy and to monitor response to therapy in breast cancer, liver metastases, and liver tumors treated with transarterial chemoembolization and radiofrequency ablation [15–17, 34–53]. Clearly there is substantial interest in the development of CEUS to diagnose and assess treatment response in the oncology population.

It is widely accepted that angiogenesis (the development of new blood vessels) is essential for tumor development, growth, and metastasis [54, 55]. Subsequently, accurate imaging and quantitation of tumor vascularity is an important area of investigation. Contrast-enhanced ultrasound is emerging as a reliable method of measuring tumor vascularity and assessing therapy response in a variety of adult malignancies [56–66]. Ultrasound contrast agents can be given in very small doses, remain in the vascular space (due to their size), and are detectable at the capillary level. With contrast-specific software programs, several CEUS time-intensity curve parameters, such as peak enhancement intensity (PI), rise time (RT), mean transit time (MTT), and area under the curve (AUC), can be quantitated. CEUS has unique attributes that make it more appealing for measuring tumor blood flow than other imaging modalities. Because UCAs remain in the vascular space, the pharmacodynamics are less complex than for CT and MR contrast agents that freely diffuse across the vascular membrane. It is less expensive than contrast-enhanced CT and MRI, can be performed at the bedside, does not require sedation, and, most importantly in the pediatric population, does not expose the patient to the potentially harmful effects of ionizing radiation.

In one study of 13 children receiving Phase 1 anti-angiogenic therapy, investigators performed quantitative, dynamic CEUS in children with recurrent solid tumors to monitor the effect of anti-angiogenic therapy. In that study a target lesion (primary or metastatic) that was amenable to ultrasound visualization was chosen for baseline and follow-up imaging. A contrast compatible transducer was placed over the largest diameter of the target lesion in either the transverse or longitudinal plane. The study subject was administered an intravenous bolus of a UCA and dynamic contrast imaging was obtained for 60 s after the injection. Using the ultrasound machine contrast-specific software, a region of interest was drawn just inside the tumor margins, and time-intensity curves were

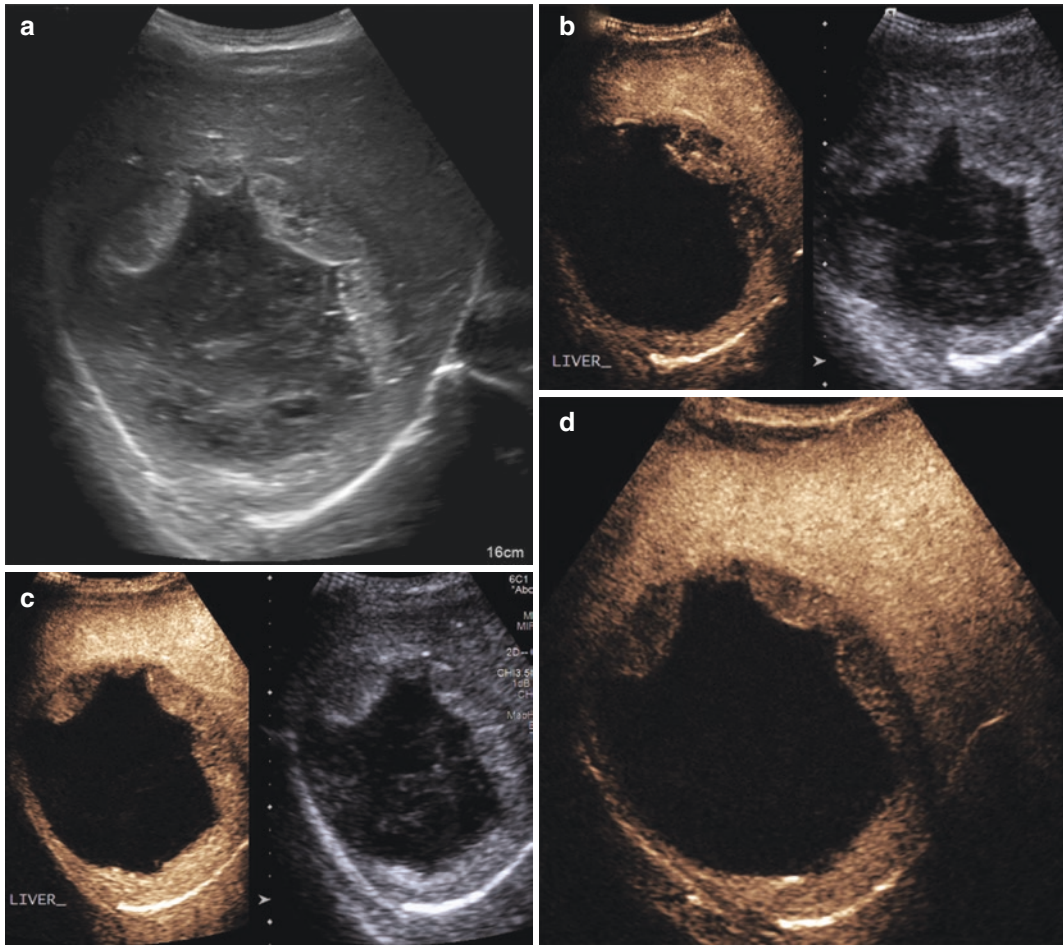

Fig. 8.6 A 10-year-old girl with undifferentiated embryonal sarcoma of the liver. (**a**) Sagittal grayscale ultrasound image shows the largely cystic primary tumor. Sagittal CEUS images (left side of panels) obtained in the (**b**) arterial phase show enhancement of the solid rim of tumor. (**c**) In the portal venous phase, there is further globular enhancement toward the center of the lesion with lack of internal enhancement. (**d**) At about 3 min after injection, there is faint, late washout in the peripheral rim. These imaging features are typical of embryonal sarcoma of the liver

obtained (Fig. 8.9). The investigators were careful to include an anatomic landmark within the field of view in order to ensure similar placement of the transducer at follow-up imaging time points (Figs. 8.10 and 8.11). From each time-intensity curve, six parameters were derived including peak enhancement (PE), rate of enhancement (RE), time to peak enhancement (TTP), total area under the curve (AUC), AUC during the first 10 s of enhancement (wash-in, AUC_1), and AUC during the second 10 s of enhancement (washout, AUC_2) (Fig. 8.9). The investigators found that the PE, RE, and AUC_1 were significantly associated with time to progression such that greater reductions in those parameters from baseline to the end of course one predicted a longer time to progression. Figures 8.10 and 8.11 show the difference in enhancement patterns between a patient with a long time to progression and a patient with a short time to progression [67]. These results are promising and warrant validation in larger clinical trials. Recent reports from the adult oncology community show that this approach is useful not only in assessing response to anti-angiogenic therapy, but to assess response to conventional chemotherapy as well [59–63, 68].

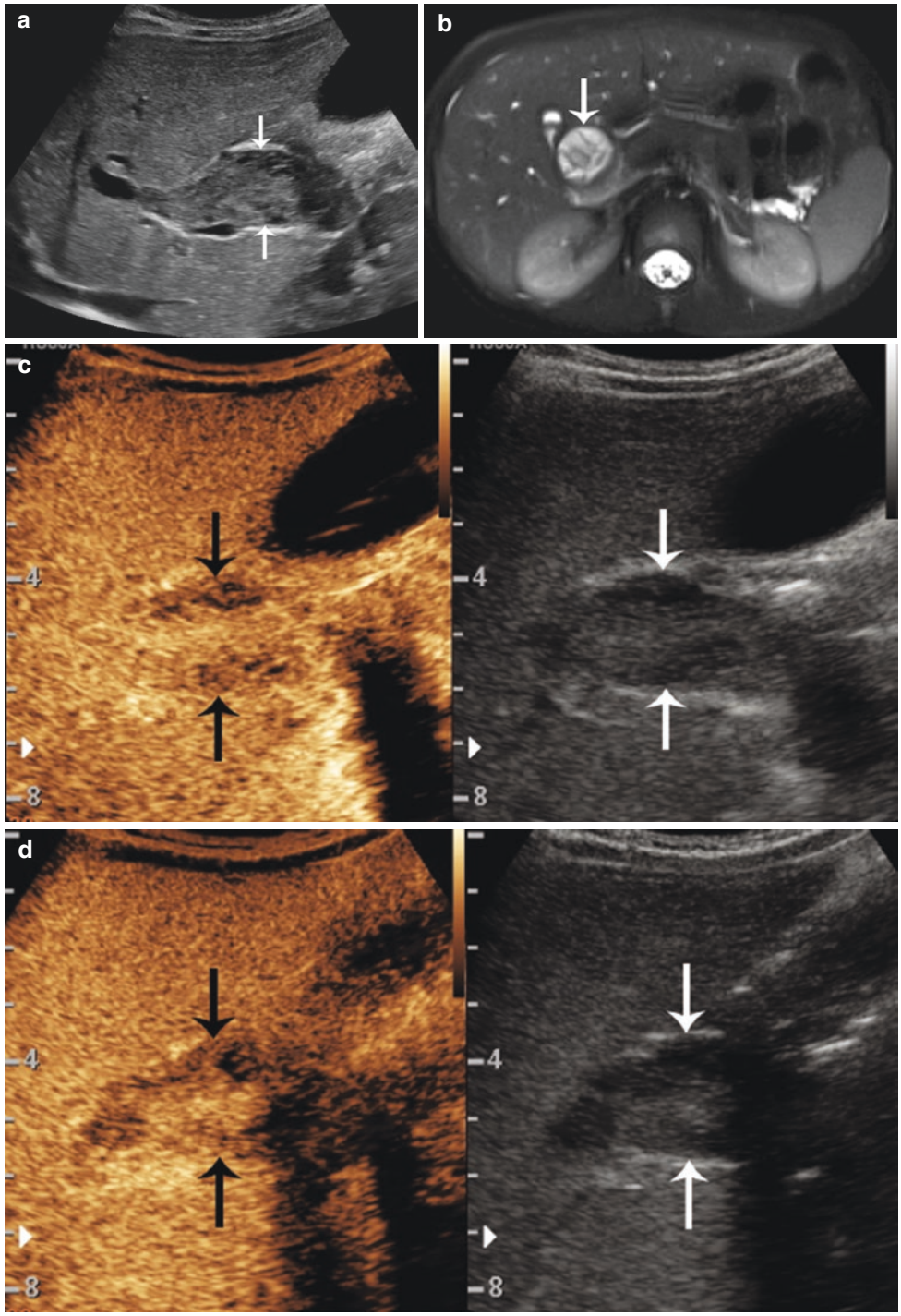

Fig. 8.7 A 5-year-old boy with rhabdomyosarcoma of the biliary tree. (**a**) Transverse grayscale ultrasound image shows tumor arising from the common bile duct (arrows). Transverse CEUS images (left side of panels) show (**b**) Transverse T2W MR image shows the tumor occupying and expanding the lumen of the common bile duct (arrows). (**c**) heterogeneous enhancement in the early arterial phase (arrows). (**d**) Early washout of contrast material at 32 s after injection (arrows)

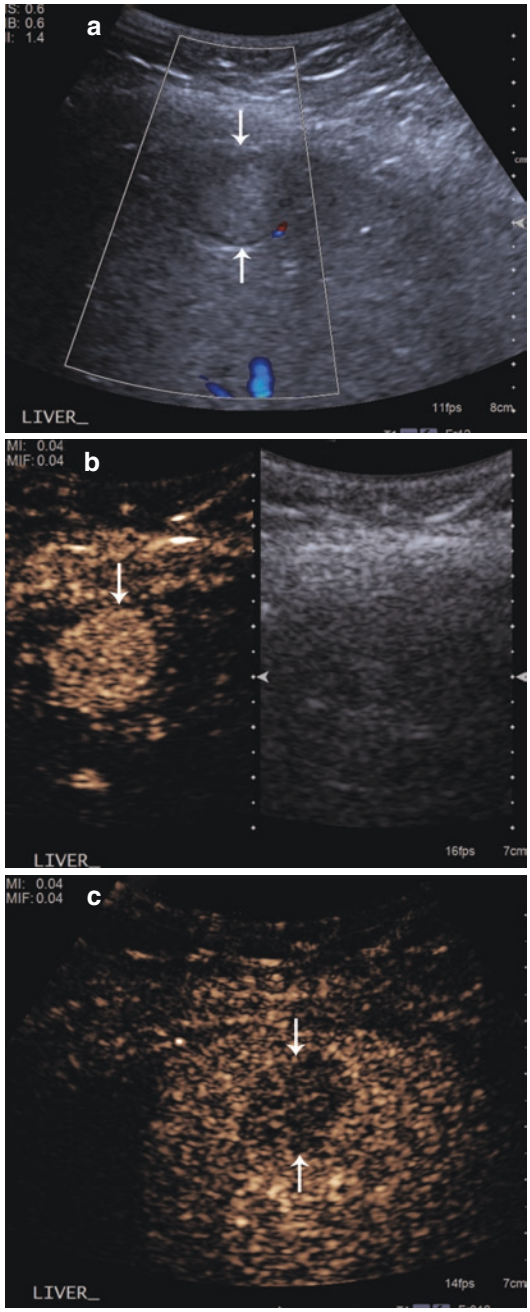

Fig. 8.8 An 11-year-old girl with metastatic pancreatic neuroendocrine tumor. (**a**) Transverse grayscale ultrasound image shows a slightly hyperechoic subcapsular lesion with a hypoechoic halo and no visible internal vascularity (arrows). (**b**) Transverse CEUS image (left side of panel) obtained in the arterial phase shows the lesion to be hyperenhancing. (**c**) This CEUS image obtained in the portal venous phase shows frank washout of the lesion (arrows). These features are consistent with a liver metastasis

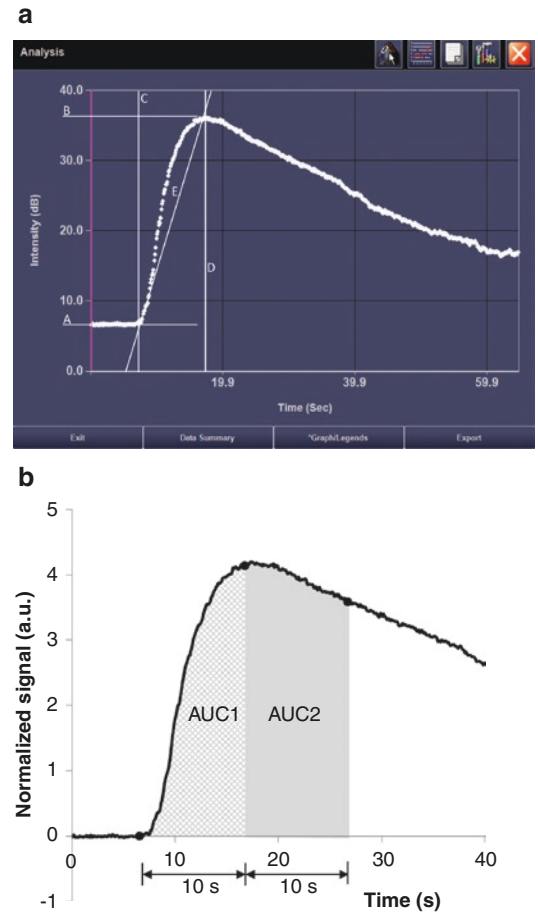

Fig. 8.9 (**a**) Time-intensity curve and parameters generated from a region of interest within the tumor shown in Fig. 8.10. (**b**) This normalized time-intensity curve for measurement of the area under the curve (AUC) was created off-line from exported raw data for the same tumor (reprinted with permission from reference [67]). *A* = baseline, pre-contrast signal (dB). *B* = maximal enhancement: peak enhancement (PE) = *B* − *A* in dB. *C* = time of arrival of contrast agent into region of interest (s). *D* = time of maximal enhancement (s): time to peak (TTP) = *D* − *C* (s). *E* = rate of change in enhancement (RE) calculated as PE/TTP in dB/s

The role of CEUS in oncology is extending beyond diagnosis and treatment monitoring into the realm of molecular imaging and targeted therapy. Numerous methods of UCA-mediated drug delivery are under investigation in preclinical and clinical trials. These include the use of microbubble contrast agents for direct and indirect drug

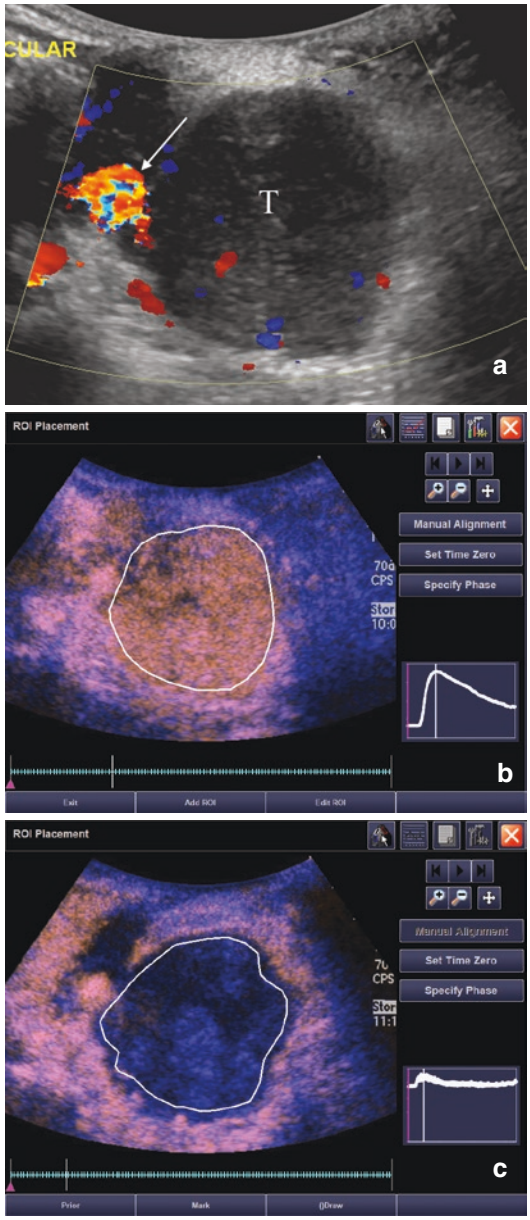

Fig. 8.10 A 15-year-old girl with recurrent synovial sarcoma. (**a**) Transverse color Doppler grayscale sonogram of the largest transverse area of a left supraclavicular tumor (T). Common carotid artery (arrow) was used as a landmark to insure similar transducer placement on follow-up studies. (**b**) Baseline CEUS with region of interest (ROI, solid line) drawn just inside tumor margins. Vertical line in the inset time-intensity curve indicates that this image was obtained at peak enhancement (PE) of 28.9 dB. (**c**) Day 7 after initiation of therapy, image obtained at PE of 2.0 dB giving a 93% reduction compared to baseline. This subject's time to progression was 242 days after initiation of therapy (reprinted with permission from reference [67])

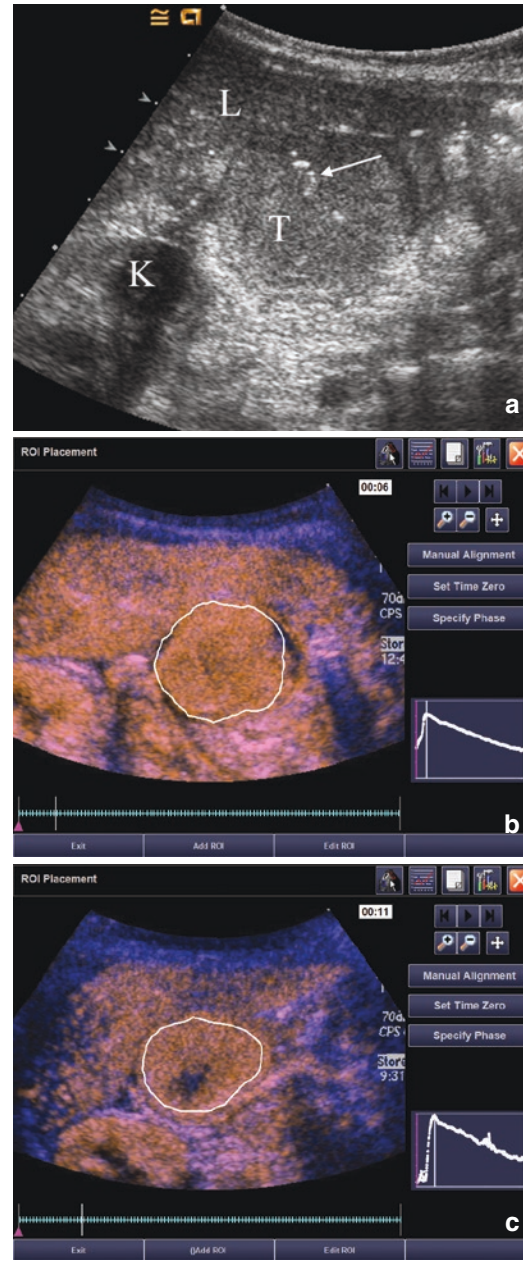

Fig. 8.11 A 21-month-old girl with recurrent rhabdoid tumor. (**a**) Transverse grayscale sonogram shows a peritoneal tumor (T) located posterior to the liver (L) and medial to the right kidney (K). Tumoral calcification (arrow) and adjacent organs were used as landmarks for transducer placement. (**b**) Baseline CEUS image with ROI inside tumor margins, obtained at PE of 33.5 dB. (**c**) Day 7 after initiation of therapy, CEUS image obtained at PE of 30.6 dB giving an 8.7% reduction compared to baseline. This subject progressed at 22 days after initiation of therapy (reprinted with permission from reference [67])

delivery and nanoscaled UCAs. Using an ultrasound pulse microbubble, UCAs can be destroyed to create micro-jets or excited to oscillate and physically massage the vascular wall to create pores in the vascular membrane. The resultant enhanced vessel permeability allows for the extravasation of co-administered drugs (indirect drug delivery). Alternatively, the microbubble shell itself can be loaded with a drug to be released during microbubble destruction which can then extravasate through the US-mediated, permeabilized vascular membrane (direct drug delivery). A limitation of this technique is the difficulty in achieving high enough doses of the therapeutic agent. The use of nanoscaled UCAs capitalizes on the fact that tumor vasculature has disorganized architecture and wider, leakier, endothelial fenestrations than normal vessels. Despite this, the relatively large UCA microbubbles cannot pass through the endothelial openings. This has led to the development of nanobubble, nanoparticle, and nanodroplet UCAs that are capable of passing through the damaged endothelium and accumulate in the extracellular space. Once in the extracellular space, they can be manipulated to coalesce and form microbubbles which can be further induced to cause tissue cavitation and to release drugs directly into the tumor. This approach could be especially advantageous in treating brain tumors by allowing the drug to pass through the blood-brain barrier. A variety of nanoscaled UCAs are currently under investigation. Although some of these agents have a short shelf life and handling difficulties, they provide promising clinical directions and exciting research opportunities [69].

8.6 Conclusions

Contrast-enhanced ultrasound is especially well suited for pediatric use because the contrast agents are safe in children, the equipment is portable, and the technique does not require prescreening laboratory testing or sedation and most importantly does not expose the patient to the harmful effects of ionizing radiation. The latter point is particularly relevant to the pediatric oncology population because these children undergo innumerable radiological examinations during diagnosis and staging, throughout treatment and during surveillance after the completion of therapy. We have presented pediatric safety data and clinical applications that support and promote the use of this modality in pediatric oncology patients. There is active ongoing research investigating the value of CEUS to quantitatively monitor the effect of therapy and as a theranostic tool in cancer treatment. We believe that these developments will significantly expand the role and increase the impact of CEUS in the management of pediatric oncology patients in the near future.

References

1. Berrington de Gonzalez A, Salotti JA, McHugh K, et al. Relationship between paediatric CT scans and subsequent risk of leukaemia and brain tumours: assessment of the impact of underlying conditions. Br J Cancer. 2016;114(4):388–94.
2. Tibussek D, Rademacher C, Caspers J, et al. Gadolinium brain deposition after macrocyclic gadolinium administration: a pediatric case-control study. Radiology. 2017;285:223.
3. Yusuf GT, Sellars ME, Deganello A, Cosgrove DO, Sidhu PS. Retrospective analysis of the safety and cost implications of pediatric contrast-enhanced ultrasound at a single center. AJR Am J Roentgenol. 2017;208(2):446–52.
4. Piskunowicz M, Kosiak W, Batko T, Piankowski A, Polczynska K, Adamkiewicz-Drozynska E. Safety of intravenous application of second-generation ultrasound contrast agent in children: prospective analysis. Ultrasound Med Biol. 2015;41(4):1095–9.
5. Coleman JL, Navid F, Furman WL, McCarville MB. Safety of ultrasound contrast agents in the pediatric oncologic population: a single-institution experience. AJR Am J Roentgenol. 2014;202(5):966–70.
6. Jacob J, Deganello A, Sellars ME, Hadzic N, Sidhu PS. Contrast enhanced ultrasound (CEUS) characterization of grey-scale sonographic indeterminate focal liver lesions in pediatric practice. Ultraschall Med. 2013;34(6):529–40.
7. Valentino M, Serra C, Pavlica P, et al. Blunt abdominal trauma: diagnostic performance of contrast-enhanced US in children--initial experience. Radiology. 2008;246(3):903–9.
8. Bonini G, Pezzotta G, Morzenti C, Agazzi R, Nani R. Contrast-enhanced ultrasound with SonoVue in the evaluation of postoperative complications in pediatric liver transplant recipients. J Ultrasound. 2007;10(2):99–106.

9. McMahon CJ, Ayres NA, Bezold LI, et al. Safety and efficacy of intravenous contrast imaging in pediatric echocardiography. Pediatr Cardiol. 2005;26(4):413–7.
10. Sidhu PS, Cantisani V, Deganello A, et al. Reply: role of contrast-enhanced ultrasound (CEUS) in paediatric practice: an EFSUMB position statement. Ultraschall Med. 2017;38:33.
11. Harkanyi Z. Potential applications of contrast-enhanced ultrasound in pediatric patients. Ultrasound Clin. 2013;2013(3):403–22.
12. Piscaglia F, Bolondi L. The safety of Sonovue in abdominal applications: retrospective analysis of 23188 investigations. Ultrasound Med Biol. 2006;32(9):1369–75.
13. McCarville MB, Kaste SC, Hoffer FA, et al. Contrast-enhanced sonography of malignant pediatric abdominal and pelvic solid tumors: preliminary safety and feasibility data. Pediatr Radiol. 2012;42(7):824–33.
14. Riccabona M. Application of a second-generation US contrast agent in infants and children--a European questionnaire-based survey. Pediatr Radiol. 2012;42(12):1471–80.
15. D'Onofrio M, Crosara S, De Robertis R, et al. Malignant focal liver lesions at contrast-enhanced ultrasonography and magnetic resonance with hepatospecific contrast agent. Ultrasound. 2014;22(2):91–8.
16. Quaia E, De Paoli L, Angileri R, Cabibbo B, Cova MA. Indeterminate solid hepatic lesions identified on non-diagnostic contrast-enhanced computed tomography: assessment of the additional diagnostic value of contrast-enhanced ultrasound in the non-cirrhotic liver. Eur J Radiol. 2014;83(3):456–62.
17. Trillaud H, Bruel JM, Valette PJ, et al. Characterization of focal liver lesions with SonoVue-enhanced sonography: international multicenter-study in comparison to CT and MRI. World J Gastroenterol. 2009;15(30):3748–56.
18. Stenzel M. Intravenous contrast-enhanced sonography in children and adolescents - a single center experience. J Ultrason. 2013;13(53):133–44.
19. Pschierer K, Grothues D, Rennert J, et al. Evaluation of the diagnostic accuracy of CEUS in children with benign and malignant liver lesions and portal vein anomalies. Clin Hemorheol Microcirc. 2015;61(2):333–45.
20. Smith EA, Salisbury S, Martin R, Towbin AJ. Incidence and etiology of new liver lesions in pediatric patients previously treated for malignancy. AJR Am J Roentgenol. 2012;199(1):186–91.
21. Dietrich CF, Maddalena ME, Cui XW, Schreiber-Dietrich D, Ignee A. Liver tumor characterization--review of the literature. Ultraschall Med. 2012;33(Suppl 1):S3–10.
22. Weinberg AG, Finegold MJ. Primary hepatic tumors of childhood. Hum Pathol. 1983;14(6):512–37.
23. Chiorean L, Cui XW, Tannapfel A, et al. Benign liver tumors in pediatric patients - review with emphasis on imaging features. World J Gastroenterol. 2015;21(28):8541–61.
24. Meyers RL. Tumors of the liver in children. Surg Oncol. 2007;16(3):195–203.
25. Yikilmaz A, George M, Lee EY. Pediatric hepatobiliary neoplasms: an overview and update. Radiol Clin North Am. 2017;55(4):741–66.
26. Roebuck DJ, Yang WT, Lam WW, Stanley P. Hepatobiliary rhabdomyosarcoma in children: diagnostic radiology. Pediatr Radiol. 1998;28(2):101–8.
27. Mork H, Ignee A, Schuessler G, Ott M, Dietrich CF. Analysis of neuroendocrine tumour metastases in the liver using contrast enhanced ultrasonography. Scand J Gastroenterol. 2007;42(5):652–62.
28. Trojan J, Hammerstingl R, Engels K, Schneider AR, Zeuzem S, Dietrich CF. Contrast-enhanced ultrasound in the diagnosis of malignant mesenchymal liver tumors. J Clin Ultrasound. 2010;38(5):227–31.
29. Liu GJ, Xu HX, Lu MD, et al. Correlation between enhancement pattern of hepatocellular carcinoma on real-time contrast-enhanced ultrasound and tumour cellular differentiation on histopathology. Br J Radiol. 2007;80(953):321–30.
30. Dietrich CF, Averkiou MA, Correas JM, Lassau N, Leen E, Piscaglia F. An EFSUMB introduction into dynamic contrast-enhanced ultrasound (DCE-US) for quantification of tumour perfusion. Ultraschall Med. 2012;33(4):344–51.
31. Al Bunni F, Deganello A, Sellars ME, Schulte KM, Al-Adnani M, Sidhu PS. Contrast-enhanced ultrasound (CEUS) appearances of an adrenal phaeochromocytoma in a child with Von Hippel-Lindau disease. J Ultrasound. 2014;17(4):307–11.
32. Ragel M, Nedumaran A, Makowska-Webb J. Prospective comparison of use of contrast-enhanced ultrasound and contrast-enhanced computed tomography in the Bosniak classification of complex renal cysts. Ultrasound. 2016;24(1):6–16.
33. Drudi FM, Valentino M, Bertolotto M, et al. CEUS time intensity curves in the differentiation between leydig cell carcinoma and seminoma: a multicenter study. Ultraschall Med. 2016;37(2):201–5.
34. Zhang Y, Luo YK, Zhang MB, Li J, Li J, Tang J. Diagnostic accuracy of contrast-enhanced ultrasound enhancement patterns for thyroid nodules. Med Sci Monit. 2016;22:4755–64.
35. Defortescu G, Cornu JN, Bejar S, et al. Diagnostic performance of contrast-enhanced ultrasonography and magnetic resonance imaging for the assessment of complex renal cysts: a prospective study. Int J Urol. 2017;24(3):184–9.
36. Wei SP, Xu CL, Zhang Q, et al. Contrast-enhanced ultrasound for differentiating benign from malignant solid small renal masses: comparison with contrast-enhanced CT. Abdom Radiol (NY). 2017;42:2135.
37. Sanz E, Hevia V, Gomez V, et al. Renal complex cystic masses: usefulness of contrast-enhanced ultrasound (CEUS) in their assessment and its agreement with computed tomography. Curr Urol Rep. 2016;17(12):89.
38. Barr RG, Peterson C, Hindi A. Evaluation of indeterminate renal masses with contrast-enhanced

US: a diagnostic performance study. Radiology. 2014;271(1):133–42.
39. Edenberg J, Gloersen K, Osman HA, Dimmen M, Berg GV. The role of contrast-enhanced ultrasound in the classification of CT-indeterminate renal lesions. Scand J Urol. 2016;50(6):445–51.
40. Putz FJ, Erlmeier A, Wiesinger I, et al. Contrast-enhanced ultrasound (CEUS) in renal imaging at an interdisciplinary ultrasound centre: possibilities of dynamic microvascularisation and perfusion. Clin Hemorheol Microcirc. 2017;66:293.
41. Liu Y, Xu Y, Cheng W, Liu X. Quantitative contrast-enhanced ultrasonography for the differential diagnosis of endometrial hyperplasia and endometrial neoplasms. Oncol Lett. 2016;12(5):3763–70.
42. Gruber L, Loizides A, Luger AK, et al. Soft-tissue tumor contrast enhancement patterns: diagnostic value and comparison between ultrasound and MRI. AJR Am J Roentgenol. 2017;208(2):393–401.
43. Guo S, Xu P, Zhou A, et al. Contrast-enhanced ultrasound differentiation between low and high-grade bladder urothelial carcinoma and correlation with tumor microvessel density. J Ultrasound Med. 2017;36:2287.
44. Cantisani V, Bertolotto M, Weskott HP, et al. Growing indications for CEUS: the kidney, testis, lymph nodes, thyroid, prostate, and small bowel. Eur J Radiol. 2015;84(9):1675–84.
45. Knieling F, Strobel D, Rompel O, et al. Spectrum, applicability and diagnostic capacity of contrast-enhanced ultrasound in pediatric patients and young adults after intravenous application - a retrospective trial. Ultraschall Med. 2016;37(6):619–26.
46. Seitz K, Strobel D. A milestone: approval of CEUS for diagnostic liver imaging in adults and children in the USA. Ultraschall Med. 2016;37(3):229–32.
47. Seitz K, Strobel D, Bernatik T, et al. Contrast-enhanced ultrasound (CEUS) for the characterization of focal liver lesions - prospective comparison in clinical practice: CEUS vs. CT (DEGUM multicenter trial). Parts of this manuscript were presented at the Ultrasound Dreilandertreffen 2008, Davos. Ultraschall Med. 2009;30(4):383–9.
48. Mori N, Mugikura S, Takahashi S, et al. Quantitative analysis of contrast-enhanced ultrasound imaging in invasive breast cancer: a novel technique to obtain histopathologic information of microvessel density. Ultrasound Med Biol. 2017;43(3):607–14.
49. Tai CJ, Huang MT, Wu CH, et al. Contrast-enhanced ultrasound and computed tomography assessment of hepatocellular carcinoma after transcatheter arterial chemo-embolization: a systematic review. J Gastrointestin Liver Dis. 2016;25(4):499–507.
50. Ishii T, Numata K, Hao Y, et al. Evaluation of hepatocellular carcinoma tumor vascularity using contrast-enhanced ultrasonography as a predictor for local recurrence following radiofrequency ablation. Eur J Radiol. 2017;89:234–41.
51. Bartolotta TV, Taibbi A, Picone D, Anastasi A, Midiri M, Lagalla R. Detection of liver metastases in cancer patients with geographic fatty infiltration of the liver: the added value of contrast-enhanced sonography. Ultrasonography. 2017;36(2):160–9.
52. Pandey P, Lewis H, Pandey A, et al. Updates in hepatic oncology imaging. Surg Oncol. 2017;26(2):195–206.
53. Granata V, Fusco R, Catalano O, et al. Diagnostic accuracy of magnetic resonance, computed tomography and contrast enhanced ultrasound in radiological multimodality assessment of peribiliary liver metastases. PLoS One. 2017;12(6):e0179951.
54. Maj E, Papiernik D, Wietrzyk J. Antiangiogenic cancer treatment: the great discovery and greater complexity (Review). Int J Oncol. 2016;49(5):1773–84.
55. Hendry SA, Farnsworth RH, Solomon B, Achen MG, Stacker SA, Fox SB. The role of the tumor vasculature in the host immune response: implications for therapeutic strategies targeting the tumor microenvironment. Front Immunol. 2016;7:621.
56. Lee SC, Grant E, Sheth P, et al. Accuracy of contrast-enhanced ultrasound compared with magnetic resonance imaging in assessing the tumor response after neoadjuvant chemotherapy for breast cancer. J Ultrasound Med. 2017;36(5):901–11.
57. Lassau N, Bonastre J, Kind M, et al. Validation of dynamic contrast-enhanced ultrasound in predicting outcomes of antiangiogenic therapy for solid tumors: the French multicenter support for innovative and expensive techniques study. Invest Radiol. 2014;49(12):794–800.
58. Atri M, Hudson JM, Sinaei M, et al. Impact of acquisition method and region of interest placement on inter-observer agreement and measurement of tumor response to targeted therapy using dynamic contrast-enhanced ultrasound. Ultrasound Med Biol. 2016;42(3):763–8.
59. Amioka A, Masumoto N, Gouda N, et al. Ability of contrast-enhanced ultrasonography to determine clinical responses of breast cancer to neoadjuvant chemotherapy. Jpn J Clin Oncol. 2016;46(4):303–9.
60. Saracco A, Szabo BK, Tanczos E, Bergh J, Hatschek T. Contrast-enhanced ultrasound (CEUS) in assessing early response among patients with invasive breast cancer undergoing neoadjuvant chemotherapy. Acta Radiol. 2017;58(4):394–402.
61. Matsui S, Kudo M, Kitano M, Asakuma Y. Evaluation of the response to chemotherapy in advanced gastric cancer by contrast-enhanced harmonic EUS. Hepatogastroenterology. 2015;62(139):595–8.
62. Peng C, Liu LZ, Zheng W, et al. Can quantitative contrast-enhanced ultrasonography predict cervical tumor response to neoadjuvant chemotherapy? Eur J Radiol. 2016;85(11):2111–8.
63. Jia WR, Tang L, Wang DB, et al. Three-dimensional contrast-enhanced ultrasound in response assessment for breast cancer: a comparison with dynamic contrast-enhanced magnetic resonance imaging and pathology. Sci Rep. 2016;6:33832.
64. Ohno N, Miyati T, Yamashita M, Narikawa M. Quantitative assessment of tissue perfusion in

hepatocellular carcinoma using perflubutane dynamic contrast-enhanced ultrasonography: a preliminary study. Diagnostics. 2015;5(2):210–8.
65. Mogensen MB, Hansen ML, Henriksen BM, et al. Dynamic contrast-enhanced ultrasound of colorectal liver metastases as an imaging modality for early response prediction to chemotherapy. Diagnostics. 2017;7(2)
66. Wu Z, Yang X, Chen L, et al. Anti-angiogenic therapy with contrast-enhanced ultrasound in colorectal cancer patients with liver metastasis. Medicine. 2017;96(20):e6731.
67. McCarville MB, Coleman JL, Guo J, et al. Use of quantitative dynamic contrast-enhanced ultrasound to assess response to antiangiogenic therapy in children and adolescents with solid malignancies: a pilot study. AJR Am J Roentgenol. 2016;206(5):933–9.
68. Ueda N, Nagira H, Sannomiya N, et al. Contrast-enhanced ultrasonography in evaluation of the therapeutic effect of chemotherapy for patients with liver metastases. Yonago Acta Med. 2016;59(4):255–61.
69. Guvener N, Appold L, de Lorenzi F, et al. Recent advances in ultrasound-based diagnosis and therapy with micro- and nanometer-sized formulations. Methods. 2017;130:4.